Noname manuscript No.
(will be inserted by the editor)

Automated error control in finite element methods with applications in fluid flow

Johan Jansson · Jeannette Spühler · Cem Degirmenci · Johan Hoffman

the date of receipt and acceptance should be inserted later

Abstract In this paper we present a new adaptive finite element method for the solution of linear and non-linear partial differential equations directly using the a posteriori error representation as a local error indicator, with the primal and dual solutions approximated in the same finite element space, here piecewise continuous linear functions on the same mesh. Since this approach gives a global a posteriori error representation that is zero due to Galerkin orthogonality, the error representation has traditionally been thought to contain no information about the error. However, for elliptic and convection-diffusion model problems we show the opposite, that locally the orthogonal error representation behaves very similar to the non-orthogonal error representation using a higher order approximation of the dual. We have previously proved an a priori estimate of the local error indicator for elliptic problems, and in this paper we extend the proof to convection-reaction problems. We also present a version of the method for non-elliptic and non-linear problems using a stabilized finite element method where the a posteriori error representation is no longer orthogonal. We apply this method to the stationary incompressible Navier-Stokes equation and perform detailed numerical experiments which show that the a posteriori error estimate is within a factor 2 of the error based on a reference value on a fine mesh, except in a few data points on very coarse meshes for a non-smooth test case where it is within a factor 3.

Keywords FEM · a posteriori · error control · adaptivity · fluid mechanics

Johan Jansson
Basque Center for Applied Mathematics, Bilbao, Spain and
CSC, KTH Royal Institute of Technology, Stockholm, Sweden
E-mail: jjan@kth.se

Jeannette Spühler
CSC, KTH Royal Institute of Technology, Stockholm, Sweden
E-mail: spuhler@kth.se

Cem Degirmenci
CSC, KTH Royal Institute of Technology, Stockholm, Sweden
E-mail: ncde@kth.se

Johan Hoffman
CSC, KTH Royal Institute of Technology, Stockholm, Sweden
E-mail: jhoffman@kth.se

1 Introduction

Partial differential equations (PDE) is one of the most fundamental models in mathematical physics. The finite element method (FEM) offers a methodology for discretisation of PDE for which a general theory for a posteriori error estimation using duality techniques has been developed since the early 1990s [8,3]. Based on a posteriori estimates of the error in a chosen output quantity, or goal functional, adaptive algorithms have been designed where the FEM discretisation is optimised with respect to this goal functional. An adaptive algoritm is based on *error indicators* over the finite element mesh that characterise the local contribution to the global error. By iteratively refining the discretisation based on the error indicators, e.g. by bisecting cells that contribute most to the global error, an efficient method can be obtained using a minimal number of degrees of freedom. A stop criterion for the adaptive algorithm can then be derived from the a posteriori estimation of the global error.

Although adaptive finite element methods (AFEM) today are used extensively in a number of different areas [14,6,1,16,13], challenges remain with respect to the generality, efficiency and reliability of the methodology. An a posteriori error estimate takes the form of an inner product involving the solution of a dual (adjoint) problem, and one key challenge of AFEM is the numerical approximation of this dual solution. In particular, since FEM is based on a Galerkin formulation of the PDE, using the same finite element spaces to approximate the primal and dual solutions makes the inner product vanish so that the a posteriori estimate of the global error is zero, which clearly is wrong. To avoid this problem one can distinguish two standard approaches: (i) either an enhanced approximation of the dual solution is computed, e.g. from using a higher order finite element space, or (ii) a projection of the dual solution on the finite element space is subtracted using Galerkin orthogonality, and then Cauchy-Schwarz inequality together with interpolation error estimates are used to bound the local error indicators in terms of derivates of the dual solution. The downside of (i) is an increased computational cost and thus a less efficient method, and (ii) leads to a lack of sharpness which influence efficiency and reliability. Both (i) and (ii) represent a loss of simplicity and thereby generality.

In [15] we presented a new adaptive finite element method that directly uses the a posteriori error representation with the same approximation spaces for the primal and the dual, here piecewise continuous linear functions on the same mesh, thus avoiding (i) and (ii). Since this approach gives a global a posteriori error estimate that is zero (due to Galerkin orthogonality), the error representation has traditionally been thought to contain no information about the error. However, for an elliptic model problem we showed the opposite, that locally, the orthogonal error representation behaves very similar to the non-orthogonal error representation (i) using a higher order approximation of the dual. We presented evidence both in the form of an a priori estimate for the local error indicator, and a detailed computational investigation showing that the two methods exhibit very similar behavior and performance, and thus confirming the theoretical prediction.

In this paper we extend these results to non-elliptic model problems and the non-linear Navier-Stokes equation, where a stabilised finite element method is used. Here the global a posteriori error estimate is no longer zero, since the stabilised method is not a pure Galerkin method, and for a convection-reaction model problem we show that both the local error indicator and the global error estimate behave similar to an error representation using the exact dual. For the Navier-Stokes case we show numerical evidence that the global a posteriori error estimate is of good quality, here within a factor 2 of the error based on a reference value on a fine mesh, except in a few data points on very coarse meshes for a non-smooth test case with where it is within a factor 3.

We argue, based on the evidence we present in this paper, that the method has the following advantages with respect to generality, efficiency and reliability:

Generality and simplicity

There is no need for manual analytical derivation and computer implementation of error estimates specific to each equation or equation class, since error indicators take a generic form. The error analysis is thus much simpler, minimal in a sense, which can make it more easily accessible, widespread and suitable for automation. For a linear stationary boundary value problem a weak solution $u \in V$ satisfies

$$r(u, v) \equiv a(u, v) - L(v) = 0, \tag{1}$$

for all test functions v in the Hilbert space V with $r(u, v)$ the weak residual, and we seek a FEM approximation $U \in V_h$ such that

$$r(U, v) = 0, \forall v \in V_h. \tag{2}$$

In the cG(1) FEM method we let the finite element space $V_h \subset V$ consist of continuous piecewise linear functions defined on a mesh $\mathcal{T}_h$. The error indicator is then simply:

$$\mathcal{E}_K^{cG(1)} = r(U, \Phi)_K \tag{3}$$

where the index K indicates restriction to the cell $K \in \mathcal{T}_h$, and $\Phi^{cG(1)} \in V_h$ is the cG(1) approximation of the dual problem, defined by

$$a(w, \Phi) = (w, \psi), \quad \forall w \in V_h, \tag{4}$$

where ψ is the Riesz representer of the goal functional $M(\cdot) = (\cdot, \psi)$.

Reliability

For a model problem we show that the error indicator generated by the method $\mathcal{E}_K^{cG(1)} = r(U, \Phi)_K$ (with a $cG(1)$ approximation of the dual Φ) converges with order $2 + d$ to the exact error indicator $\mathcal{E}_K = r(U, \phi)_K$ (using the exact dual ϕ):

$$\|\mathcal{E}(x) - \mathcal{E}^{cG(1)}(x)\|_{L_2} \leq Ch^{2+d} \tag{5}$$

where $\mathcal{E}(x)$ and $\mathcal{E}^{cG(1)}(x)$ are piecewise constant functions over the mesh $\mathcal{T}_h$.
This indicates that the method is *reliable*, in the sense that we can control the error, which is also verified by a detailed computational study presented in figures 3-10.

Efficiency

The adaptive algorithm does not require the computation of additional constructs such as jump terms or the solution of local problems, typically generated as part of standard a posteriori error estimates, which can be costly and complex to compute, especially in a parallel programming model over distributed data.

2 A posteriori error estimation

Following the standard framework developed by Eriksson & Johnson [10,8,9] and Becker & Rannacher [4,2], with co-workers, for a linear PDE approximated by a Galerkin finite element method we can express the error in an output of interest, or goal functional, in terms of the weak residual acting on the solution of a dual (adjoint) problem ϕ:

$$M(u) - M(U) = r(U, \phi), \tag{6}$$

where ϕ in general is not available and thus needs to be approximated. If the same finite element space is used to compute approximation ϕ and U, the error representation is zero which follows from (2). We now describe the two main approaches used to bypass this problem.

2.1 Local analytical error bounds

The Galerkin orthogonality can be used to subtract a projection of the dual solution on the finite element space $\pi_h\phi \in V_h$, then asumming sufficient regularity one can use integration by parts to reformulate the error representation in terms of the strong residual and use Cauchy-Schwarz inequality and interpolation error estimates to bound the error in terms of the local mesh size $h = h(x)$, the strong residual $R(U)$ and derivatives of the dual solution.

That is, we can write:

$$|M(u) - M(U)| = |(R(U), \phi - \pi_h\phi)_{L_2(\Omega)}| = |\sum_{K\in\tau_h} (R(U), \phi - \pi_h\phi)_{L_2(K)}| \tag{7}$$

Where u is the exact solution, U is the computed solution, M is the functional for the quantity of interest, $R(U)$ is the strong residual with possible interior facet jump contributions and ϕ is the solution of the dual problem. Here Ω is the domain for the partial differential equation and $\mathcal{T}_h$ is its triangulation that is also used for constructing the finite elements space. One can observe that using an approximation of ϕ from the same FE space as the primal problem at first glance does not appear to make sense since the resulting error representation will be zero due to the Galerkin orthogonality (however, as we will see later in this paper, we show that the opposite is true and that this has very good approximation properties).

But using the Galerkin orthogonality, one can proceed with the Cauchy-Schwarz estimate to bound the error in the quantity of interest as:

$$|M(u - U)| = |\sum_{K\in\tau_h} (R(U), \phi - \pi_h\phi)_{L_2(K)}| \leq \sum_{K\in\tau_h} \|R(U)\|_{L_2(K)}\|\phi - \pi_h\phi\|_{L_2(K)} \tag{8}$$

At this point one may also use interpolation estimates to derive estimates including $D^n\phi$ derivatives of ϕ of some order [5,9]. One may compute an approximation of $\|\phi-\pi_h\phi\|_{L_2(\Omega)}$ or derivatives of ϕ if interpolation estimates are used.

Using the computed dual solution in the same FE space as the primal solution for approximating $\|\phi - \pi_h\phi\|_{L_2(K)}$ or $\|D^n\phi\|_{L_2(K)}$ now appears to make sense since the mechanism generating the orthogonality has been removed.

2.2 Enhanced dual approximation

Another approach is to compute the dual solution using a FE space that is different than the space used for approximating the primal problem. This way the Galerkin orthogonality doesn't render the approximation of ϕ with a computed dual invalid. Many choices for choosing the FE space of the dual problem are possible as listed in [12], including using a FE space with higher degree of polynomials, a FE space that is using a supermesh obtained by global refinement, or refined adaptively by an a posterori estimate of the dual problem for the same degree of polynomials or even a higher degree of polynomials if $hp-$adaptivity can be applied. These methods clearly increase the computational cost which can be avoided by computing the dual problem using the same FE space as the primal problem, but using patch-wise higher order interpolation inside (8) as mentioned in [3] and [18], which on the other hand increases the complexity of the algorithm.

3 Method description: representation adaptivity

We begin by describing the representation adaptivity method for a linear stationary model problem which allows us to perform a priori error estimation. In section 3.6 we show an extension to non-linear stationary problems in general and in section 4.2 we apply the framework to the stationary incompressible Navier-Stokes equations and evaluate the performance of the method.

3.1 Convection-diffusion-reaction model problem

We choose a convection-diffusion-reaction model problem with α and ϵ scalar coefficients representing reaction and diffusion respectively, and β a vector coefficient representing the convective velocity. The model problem in weak form reads: find $u \in V$ such that

$$r(u,v) = (\alpha u, v) + (\epsilon \nabla u, \nabla v) + (\beta \cdot \nabla u, v) - (f, v) = 0, \quad \forall v \in V \tag{9}$$

with the standard space $V = H_g^1(\Omega),\ \Omega \subset R^2$ and g data on the boundary Γ. $(\cdot,\cdot) = (\cdot,\cdot)_{L_2}$ is the L_2 inner product, with $L_2 = L_2(\Omega)$ the space of square-integrable functions in Ω.

Choosing $\beta = 0$ we obtain an elliptic model problem which we occasionally use below to simplify the analysis, where we clearly specify when we do so.

3.2 Stabilized finite element method

We solve the model problem with a Galerkin/least-squares (GLS) stabilized finite element method with continuous piecewise linear basis functions (cG(1)), that is we seek the FE solution $U \in V_h \subset V$ with V_h defined using a simplicial tesselation $\mathcal{T}_h$ of Ω with h the maximum edge length in cell K_j. But instead of requiring $r(U,v) = 0, \forall v \in V_h$, we require $r_S(U,v) = r(U,v) + (\delta R(U), R(v) + f) = 0, \forall v \in V_h$ with $R(U)$ the strong residual and δ a stabilization parameter defined as below. For the convection-diffusion-reaction model

problem the method reads: find $U \in V_h$ such that

$$\begin{aligned} r_S(U,v) = (\alpha U, v) + (\epsilon \nabla U, \nabla v) + (\beta \cdot \nabla U, v) - (f, v) + \\ (\delta(\alpha U + \beta \cdot \nabla U - f), \alpha v + \beta \cdot \nabla v) = 0, \quad \forall v \in V_h, \\ \delta = \begin{cases} \frac{h}{|\beta|}, h \geq \epsilon \\ \frac{h^2}{|\beta|}, h < \epsilon \end{cases} \end{aligned} \tag{10}$$

For the elliptic model problem with $\beta = 0$ no stabilization is needed, so we put $\delta = 0$.

3.3 A posteriori error estimation

We decompose the residual $r(U,v)$ into bilinear and linear forms where:

$$r(U,v) = a(U,v) - L(v) \tag{11}$$
$$r_S(U,v) = a_S(U,v) - L_S(v) \tag{12}$$

and:

$$\begin{aligned} L(v) &= -r(0,v) \\ a(U,v) &= r(U,v) + L(v) \\ L_S(v) &= -r_S(0,v) \\ a_S(U,v) &= r_S(U,v) + L_S(v) \end{aligned} \tag{13}$$

and we define the error e as:

$$e = u - U \tag{14}$$

By linearity:

$$-r(U,v) = r(u,v) - r(U,v) = a(u,v) - L(v) - a(U,v) + L(v) = a(e,v), \quad \forall v \in V \tag{15}$$

using that $V_h \subset V$.

We are interested in bounding the error in a linear functional $M(e) = (e, \psi)$ which we refer to as the "output quantity" by a tolerance TOL:

$$|M(u) - M(U)| = |M(e)| = |(e,\psi)| < TOL \tag{16}$$

3.3.1 Dual problem

We introduce the dual problem with solution ϕ and ψ as source term:

$$a(w,\phi) = (w,\psi), \quad \forall w \in V \tag{17}$$

noting that we have switched the order of the arguments in the bilinear form $a(\cdot,\cdot)$.

A discrete approximation Φ to the dual solution is computed with the same stabilized method as for the primal problem:

$$a_S(w,\Phi) - (w,\psi) = 0, \quad \forall w \in V_h, \quad \Phi \in V_h \tag{18}$$

3.3.2 A posteriori error representation

By (15) and (17) we can express the error in the output quantity exactly by the residual and the dual solution:

$$(e, \psi) = a(e, \phi) = -r(U, \phi) \tag{19}$$

An error estimate can trivially be stated which reads:

$$|(e, \psi)| = |r(U, \phi)| \tag{20}$$

3.4 Adaptive error control

We are now ready to use our a posteriori error estimate to control the error in our finite element approximation by adaptive mesh refinement.

To be able to compute the error estimate, we need to approximate also the dual solution by a finite element discretization with the discrete dual solution Φ from (17), the approximate a posteriori error estimate becomes:

$$|r(U, \Phi)| \tag{21}$$

Having the exact dual, our adaptive method would be based on satisfying:

$$|(e, \psi)| = |r(U, \phi)| \leq TOL \tag{22}$$

Using the computable error estimate (21) the error control is instead based on satisfying:

$$|r(U, \Phi)| \leq TOL \tag{23}$$

3.4.1 Error indicator

To be able to decide which cells in the mesh $\mathcal{T}$ to refine, we write the error estimate as a sum over all cells:

$$|r(U, \Phi)| = |\sum_{j=1}^{M} r(U, \Phi)_{K_j}| \tag{24}$$

with M the number of cells in the mesh.

We denote this cell-based quantity as the *error indicator* $\mathcal{E}_K$, with the $cG(1)$ superscript indicating that the dual solution is approximated using cG(1) finite elements:

$$\mathcal{E}_K = r(U, \phi)_K \tag{25}$$

$$\mathcal{E}_K^{cG(1)} = r(U, \Phi)_K \tag{26}$$

The error indicator can also be represented as a function in space $\mathcal{E}^{cG(1)}(x)$ by expansion in piecewise discontinuous constant basis functions $\theta \in W_h$ (θ_i = 1 in cell K_i, and 0 in all other cells):

$$\mathcal{E}^{cG(1)}(x) = \sum_{j=1}^{M} \mathcal{E}_{K_j}^{cG(1)} \theta_j(x) = \sum_{j=1}^{M} r(U, \Phi)_{K_j} \theta_j(x) \tag{27}$$

We denote $\mathcal{E}^{cG(1)}(x)$ as the *error indicator function*.

3.4.2 Adaptive mesh refinement algorithm

Based on the error indicator we can now form adaptive algorithms for how to construct finite element meshes optimized to control the error in the functional $M(U)$.

Starting from an initial coarse mesh $\mathcal{T}^0$, one simple such algorithm takes the form: let $k = 0$ then do

Algorithm 1 *Adaptive mesh refinement*

1. *For the mesh $\mathcal{T}^k$: compute the primal problem and the dual problem.*
2. *If $|\sum_{j=1}^{M} \mathcal{E}_{K_j}^{cG(1)}| < TOL$ or $|M(U^k) - M(U^{k-1})| < \gamma * TOL$ then stop, else:*
3. *Mark some chosen percentage of the elements with highest $\mathcal{E}_{K_j}^{cG(1)}$ for refinement.*
4. *Generate the refined mesh $\mathcal{T}^{k+1}$ (by e.g. Rivara bisection [17]), set $k = k+1$, and goto 1.*

with the second stopping condition $|M(U^k) - M(U^{k-1})| < \gamma * TOL$ being used for the case of an orthogonal error representation.

3.5 A priori error estimate of the error indicator

We now derive an a priori estimate for the error indicator with cG(1) approximation of the dual solution for both the elliptic ($|\beta| = 0$) and the convection-reaction ($\epsilon = 0$) model problem. We show that even though the *global error estimate* is zero: $|r(U, \Phi)| = 0$, the *error indicator function* $\mathcal{E}^{cG(1)}(x)$ (and thus the error indicators it's composed of) is of good quality and converges to the exact error indicator function $\mathcal{E}(U, \phi)(x)$ with order 2 + d, with d the geometric dimension for the elliptic case and for the convection-reaction case if the solution is smooth. For the convection-reaction case with non-smooth solution we show convergence of order $2 + d^{1/2}$.

The key to this analysis is the realization that even if the error representation is globally zero: $|r(U, \Phi)| = 0$, the L_2-norm of the *error indicator function* is not: $\|\mathcal{E}^{cG(1)}(x)\|_{L_2} > 0$, unless the function itself is zero everywhere, which is not a relevant case, since it corresponds to the exact solution.

3.5.1 Standard estimates

We recall some standard estimates which will be used in the derivation of an a priori error estimate for the cG(1) error indicator $\mathcal{E}^{cG(1)}(U, \Phi)(x)$, see e.g. [9, 7]:

A basic estimate of the L_2-projection Pf of a function f onto the space W_h:

$$\|Pf\|_{L_2} \leq \|f\|_{L_2} \tag{28}$$

And the standard interpolation estimates for the piecewise linear interpolant $\pi_h^{cG(1)} f$:

$$\|f - \pi_h^{cG(1)} f\|_{L_2} \leq C_i h^2 \|D^2 f\|_{L_2} \tag{29}$$

3.5.2 Standard estimates for the elliptic model problem

In the elliptic case the following a priori estimate in the L_2 norm can be derived [9] with Φ a cG(1) approximation of the dual solution ϕ:

$$\|\phi - \Phi\|_{L_2} \leq C_i h^2 \|D^2\phi\|_{L_2} \tag{30}$$

with h the maximum mesh size and with C_i an interpolation constant, and one can prove the following a posteriori estimate in the L_2 norm [9]:

$$\|\phi - \Phi\|_{L_2} \leq C_i h^2 \|R_\Sigma(\Phi)\|_{L_2} \tag{31}$$

with $R_\Sigma(\Phi)$ denoting the sum of all contributions to the residual expression including jump terms.

Using (30) and (31) and elliptic regularity we see that the residual must be bounded by a constant independent of h, or else (30) cannot be true:

$$\|R_\Sigma(\Phi)\|_{L_2} \leq C_R \tag{32}$$

which is also true for the primal solution U since the problem is self-adjoint.

3.5.3 Standard estimates for the non-elliptic model problem

For the stabilized reaction-convection model problem one can show the following a priori estimate in the L_2-norm [9]:

$$\|\phi - \Phi\|_{L_2} \leq C_i h^{3/2} \|D^2\phi\|_{L_2} \tag{33}$$

and an a posteriori estimate in the L_2 norm [9]:

$$\|\phi - \Phi\|_{L_2} \leq C_i h^{3/2} \|R_\Sigma(\Phi)\|_{L_2} \tag{34}$$

A basic "worst-case" estimate for the residual with a non-smooth solution based on the stabilization, using that $\delta = h$ is [9]:

$$\|R_\Sigma(\Phi)\|_{L_2} \leq C_R h^{-1} \tag{35}$$

3.5.4 Estimate of the residual for the non-elliptic model problem

We now derive an upper bound for $\|R_\Sigma(\Phi)\|_{L_2}$ for the stabilized reaction-convection model problem, for a smooth solution, which is equal to the strong residual $\|R(\Phi)\|_{L_2}$ since $\epsilon = 0$. The analysis is conducted for the primal problem but can be easily transfered to the dual case. Since $U, \pi^{cG(1)}u \in V_h$ and $R(U - \pi^{cG(1)}u) = R(U) - R(\pi^{cG(1)}u) - f$ due to $R(\cdot)$ being an affine function, (10) can be rewritten as

$$\begin{aligned} 0 &= (R(U), v) + (\delta R(U), R(v) + f) \\ &= (R(U), U - \pi^{cG(1)}u) + (\delta R(U), R(U) - R(\pi^{cG(1)}u)) \end{aligned} \tag{36}$$

with $v \in V_h$.

Thus

$$||\delta^{1/2}R(U)||_{L_2}^2 = ||(\delta R(U), R(\pi^{cG(1)}u)) - (R(U), U - \pi^{cG(1)}u)||_{L_2} \Rightarrow$$
$$||\delta^{1/2}R(U)||_{L_2} \leq ||\delta^{1/2}R(\pi^{cG(1)}u)||_{L_2} + ||U - \pi^{cG(1)}u||_{L_2} \quad (37)$$

The respective contributions on the right hand side can be estimated as

$$\begin{aligned} ||U - \pi^{cG(1)}u||_{L_2} &= ||(U - u + u - \pi^{cG(1)}u)||_{L_2} \\ &\leq ||U - u||_{L_2} + ||u - \pi^{cG(1)}u)||_{L_2} \\ &\leq C_1 h^{3/2}\|D^2 u\|_{L_2} + C_2 h^2 \|D^2 u\|_{L_2} \end{aligned} \quad (38)$$

$$\begin{aligned} ||R(\pi^{cG(1)}u)||_{L_2} &= ||\alpha\pi^{cG(1)}u + \beta \cdot \nabla \pi^{cG(1)}u - f||_{L_2} \\ &= ||\alpha(\pi^{cG(1)}u - u) + \beta \cdot \nabla(\pi^{cG(1)}u - u)||_{L_2} \\ &\leq C_3 h^2 \|D^2 u\|_{L_2} + C_4 h \|D^2 u\|_{L_2} \end{aligned} \quad (39)$$

again with $\delta = h$.

Thus, we can conclude that

$$\|R_\Sigma(\Phi)\|_{L_2} \leq C_R h^{1/2} \quad (40)$$

3.5.5 Derivation of the a priori estimate

We begin by re-arranging our error indicator expressions:

$$\begin{aligned} \|\mathcal{E}(x) - \mathcal{E}^{cG(1)}(x)\|_{L_2} &= \|\sum_{j=1}^{M} r(U,\phi)_{K_j}\theta_j(x) - \sum_{j=1}^{M} r(U,\Phi)_{K_j}\theta_j(x)\|_{L_2} \\ &= \|\sum_{j=1}^{M} r(U,\phi-\Phi)_{K_j}\theta_j(x)\|_{L_2} \end{aligned} \quad (41)$$

We then use a projected form of the residual (a projection of the jump terms coming from the viscous term, see [15]) to separate out the error in the dual solution ϕ.

$$\|\sum_{j=1}^{M} r(U,\phi-\Phi)_{L_2(K_j)}\theta_j(x)\|_{L_2} = \|\sum_{j=1}^{M} (R_\Sigma(U),\phi-\Phi)_{L_2(K_j)}\theta_j(x)\|_{L_2} \quad (42)$$

We note that the L_2-projection Pf of a function f onto the space of piecewise constants W_h can be written as:

$$Pf = \sum_{j=1}^{M} \frac{1}{|K_j|}\int_{K_j} f dx \theta_j(x) \quad (43)$$

Writing out the inner product as an integral, we thus see that we have the L_2-projection of the integrand $R_\Sigma(U)(\phi - \Phi)$ onto the space of piecewise constants W_h weighted by the piecewise constant cell volume $|K| = |K(x)|$:

$$\|\sum_{j=1}^{M} \int_{K_j} R_\Sigma(U)(\phi-\Phi)dx\theta_j(x)\|_{L_2} = \||K|P(R_\Sigma(U)(\phi-\Phi))\|_{L_2} \quad (44)$$

Using (28) and $|K| \leq C_K h^d$ with d the geometric dimension gives:

$$\||K|P(R_\Sigma(U)(\phi - \Phi))\|_{L_2} \leq C_K h^d \|R_\Sigma(U)(\phi - \Phi)\|_{L_2} \tag{45}$$

Continuing with Cauchy-Schwartz we get:

$$C_K h^d \|R_\Sigma(U)(\phi - \Phi)\|_{L_2} \leq C_K h^d \|R_\Sigma(\Phi)\|_{L_2} \|\phi - \Phi\|_{L_2} \tag{46}$$

Now, for the elliptic model problem we use (30) and (32) and define the constant C as

$$C_i C_K \|D^2 \phi\|_{L_2} \|R_\Sigma(\Phi)\|_{L_2} \leq C \tag{47}$$

In the reaction-convection model problem we apply (33) and (40) and use the same C to collect the constants.

In both cases, for a smooth solution, we then have the sought-after a priori estimate for the cG(1) error indicator $\mathcal{E}^{cG(1)}(U, \Phi)(x)$:

$$\|\mathcal{E}(x) - \mathcal{E}^{cG(1)}(x)\|_{L_2} \leq C h^{2+d} \tag{48}$$

For a non-smooth solution using (35) we have for the convection-reaction model problem:

$$\|\mathcal{E}(x) - \mathcal{E}^{cG(1)}(x)\|_{L_2} \leq C h^{1/2+d} \tag{49}$$

3.6 Extension to non-linear stationary problems

The method generalizes to non-linear stationary problems. We define the weak residual for a nonlinear problem

$$r(U; v) = 0, \quad \forall v \in V \tag{50}$$

where $r(\cdot;\cdot)$ may be nonlinear in the arguments preceding the semi-colon, but linear in the arguments following the semi-colon. We use the notation that $f'(u; w, v)$ is the derivative $D_u f(u; v)[w]$ in the direction w.

We follow the standard technique in the field [11,18] by choosing a linearization of r in a mean value sense of the exact solution u and finite element solution U:

$$\overline{r'}(w, v) = \int_0^1 r'(su + (1 - s)U; w, v) ds \tag{51}$$

This allows us to obtain the error representation:

$$(e, \psi) = \overline{r'}(e, \phi) = r(U; \phi) \tag{52}$$

As for the linear case, the dual problem for the dual solution ϕ with the functional ψ as source is defined as:

$$\overline{r'}(w, \phi) = (w, \psi), \quad \forall w \in V \tag{53}$$

A discrete approximation Φ to the dual solution is computed with the same stabilized method as for the primal problem:

$$\overline{r'_S}(w, \Phi) - (w, \psi) = 0, \quad \forall w \in V_h, \quad \Phi \in V_h \tag{54}$$

The adaptive method then has to satisfy the a posteriori error estimate:

$$|r(U;\Phi)| \leq TOL \tag{55}$$

and the error indicator is defined as:

$$\mathcal{E}_K = r(U;\phi)_K \tag{56}$$

$$\mathcal{E}_K^{cG(1)} = r(U;\Phi)_K \tag{57}$$

again with the $cG(1)$ superscript indicating that the dual solution is approximated using cG(1) finite elements.

Since we don't have access to the exact solution u, the linearization $\overline{r'}$ is approximately evaluated at the finite element solution U in (51). We do not consider the linearization error in this error estimate, but refer to [3] for a framework how to proceed in this direction.

4 Computational results

We present computational studies for two equations. First, for completeness, we include previous results from [15] for the linear stationary convection-diffusion-reaction equation from the model problem with small diffusion to illustrate the a priori estimate for the error indicator for convection-reaction. Second we present a new study of the non-linear stationary incompressible Navier-Stokes equation illustrating the extension to non-linear problems and the generality of the methodology.

4.1 Specific problem statement for convection-diffusion-reaction

We repeat the model problem formulation (9) from above :

$$r(u,v) = (\alpha u, v) + (\epsilon \nabla u, \nabla v) + (\beta \cdot \nabla u, v) - (f, v) = 0, \quad \forall v \in V$$

with the standard space $V = H_g^1(\Omega)$, $\Omega \subset R^2$ and g data on the boundary Γ. The domain is chosen to be a square with a hole in the center:

$$\Omega = (0,0) \times (1,1) \setminus (0.48, 0.48) \times (0.52, 0.52) \tag{58}$$

The data g is chosen to be $g = 0$ on the outer boundary and $g = 10$ on the inner hole boundary.

The convective velocity β is constant and chosen so as not to be aligned with the cells in a uniform mesh:

$$\beta = (-1, -0.61) \tag{59}$$

The other coefficients in the equation are varied to generate a range of test problems, and are stated in the test problem list below.

The output functional is chosen as a Gaussian function concentrated in the lower-left quadrant:

$$\psi = exp(-20|x - (0.25, 0.25)|^2) \tag{60}$$

We choose ψ smooth to avoid special treatment of possible discontinuities.

We choose the source term zero: $f = 0$, and we choose the parameters $\alpha = 1, \epsilon = 10^{-5}, |\beta| = 1.171$, a convection-dominated test problem where the error representation is non-orthogonal for the "rep" method due to stabilization. The geometry and a sample solution is shown in figure 4.1. The graphs of convergence and performance indices are plotted in figure 8. The solution, dual and mesh are plotted in figure 9, and the error indicator for adaptive iteration 0 and 10 are plotted in figure 10

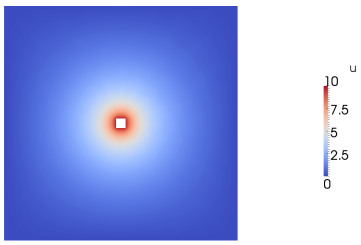

Fig. 1 The geometry and sample solution for the convection-diffusion-reaction test problem.

We present a detailed computational study comparing the $cG(1)$ representation adaptivity method ("rep") against the $cG(2)$ representation adaptivity method ("quad"), a standard Cauchy-Schwartz based adaptive method with projected jump terms and first order interpolation ("jump"), second order interpolation ("jump2") and uniform mesh refinement ("uniform"). For the adaptive methods we refine 10% of the marked cells in each adaptive iteration.

We use the "jump2" solution on the finest mesh as the reference solution, since the method is standard, robust and well-proven (see e.g. [9]).

4.2 Specific problem statement for incompressible Navier-Stokes

The second non-linear equation is the stationary incompressible Navier-Stokes equation in 2D with constant kinematic viscosity $\nu > 0$, enclosed in $\Omega \subset \mathbb{R}^2$, with boundary Γ, which takes the weak form:

$$r(\hat{u}, \hat{v}) = ((u \cdot \nabla)u + \nabla p, v) + (\nu \nabla u, \nabla v) - (f, v) + (\nabla \cdot u, q) = 0, \quad (61)$$
$$\forall v \in \hat{V}, x \in \Omega,$$
$$\hat{u} = (u, p)$$
$$\hat{v} = (v, q)$$
$$\hat{V} = \{\hat{v} \in [H^1(\Omega)]^3\} \quad (62)$$

and strong form:

$$R(\hat{u}) = \begin{cases} (u \cdot \nabla)u + \nabla p - \nu \Delta u - f = 0 \ , & x \in \Omega, \\ \nabla \cdot u = 0 \ , & x \in \Omega \end{cases}$$
$$\hat{u} = (u, p) \quad (63)$$

with $x = (x_0, x_1)$ the spatial coordinate vector, $u(x)$ the velocity vector, $p(x)$ the pressure and $f(x)$ a body force.

Again we solve the problem with a Galerkin/least-squares (GLS) stabilized finite element method with continuous piecewise linear basis functions (cG(1)), that is we require $r_S(U;v) = r(U;v) + (\delta R(U), R(v) + f) = 0, \forall v \in \hat{V}_h$.

The domain is a 2D channel:

$$\Omega = (0,0) \times (2.2, 0.41) \tag{64}$$

with a square or cylinder-shaped hole as obstacle of diameter 0.1 with center point at $(0.2, 0.2)$, denoted as "square" and "cyl" in the figures. The "cyl" geometry is displayed in figure 2.

For boundary data, we specify an inflow condition $u(x) = (4(x_1 - 0.4)/0.41^2, 0.0), x_0 \leq 0.0$, a no-slip condition $u(x) = (0.0, 0.0), 0.0 \leq x_0 \leq 2.2$ and an outflow condition $p(x) = 0.0, x_0 \geq 0.0$.

Two goal functionals are chosen as input to the adaptive method: a "pressure drag" goal functional:

$$M_{pdrag} = \int_{\Gamma_o} p n_0 ds \tag{65}$$

with Γ_o the boundary of the obstacle, representing the pressure part of the drag force and a "weighted mean velocity" goal functional:

$$M_{umean} = \int_{\Omega} g \cdot u dx \tag{66}$$

$$g(x) = (200exp(-200|x - (0.5, 0.3)|^2), 0) \tag{67}$$

representing the mean velocity weighted by a Gaussian function to localize the goal to a region near the point $(0.5, 0.3)$.

We present a detailed computational study for the representation adaptivity method applied to the "cyl" and "square" cases, for $\nu = 5 \times 10^{-3}$ and $\nu = 10^{-2}$. We run the method for 20 adaptive iterations and plot the error estimate and "error" where we compare against a reference value on a fine mesh which we get by running the method for 35 adaptive iterations. The effectivity index $\frac{|r(U,\Phi)|}{|M(e)|}$ is also plotted. We also plot the velocity U, the dual solution Φ, the error indicator function $\mathcal{E}(U, \Phi^{cG(1)})(x)$ and the mesh for adaptive iteration 0, 6 and 18.

These figures are presented for the "cyl" case with the M_{pdrag} goal functional and $\nu = 10^{-2}$ in figure 3, for $\nu = 5 \times 10^{-3}$ in figure 4. The "square" case with M_{pdrag} goal functional and $\nu = 10^{-2}$ is presented in figure 6 and with $\nu = 5 \times 10^{-3}$ in figure 7. We also present a comparison between the M_{pdrag} and M_{umean} goal functionals with $\nu = 10^{-2}$ in figure 5.

5 Discussion and conclusion

In this paper we have investigated an adaptive finite element method where we directly use the error representation as error indicator, and compute the dual solution in the same space as the primal (both cG(1)). We denote the method "cG(1) representation adaptivity" since we directly use the cG(1) error representation as error indicator. This approach has traditionally

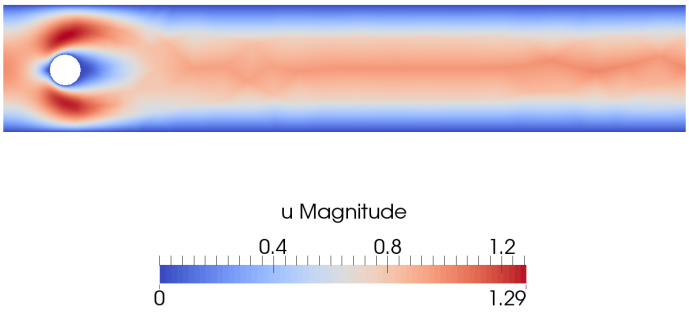

Fig. 2 The geometry and sample solution for the test problems.

been discarded a priori since the error representation is orthogonal and equal to zero, and thus has been thought to contain no information. We have shown the opposite by an a priori estimate of the error indicator and a detailed computational study, showing that the error indicator defined by the orthogonal error representation is very close to the to the error indicator defined by the non-orthogonal error representation using a quadratic approximation of the dual. For extension to non-linear problems we can use the same approach described in [18].

Specific conclusions we can derive from the results are:

Convergence of the cG(1) error indicator
: The cG(1) orthogonal error indicator converges to the exact error indicator (with exact dual) with order $2 + d$ with d the geometric dimension. We prove this in the a priori estimate (48). The elliptic case (only diffusion) was done in [15] and here we extend the proof to the convection-reaction case.

Similar behavior between the cG(1) and cG(2) error indicators
: The detailed computational study for the convection-reaction-diffusion case presented in figure 10 shows that the plots of the adaptively generated meshes, error and error estimates are very similar, a close visual inspection is needed to see differences in the meshes for example.

Good quality error estimate of the cG(1) error indicator with stabilization
: Using the cG(1) error indicator for a stabilized method no longer gives an orthogonal error representation and indicator. Since we have shown that the error indicator is of very good quality (aside from the orthogonality making the estimate 0) in the a priori estimates for elliptic and convection-reaction problems, we expect the error estimate in the stabilized case to also be of good quality. In figures 3-7 corresponding to the stabilized method for stationary incompressible Navier-Stokes we can verify that this is the case, with the effectivity index for all cases in the interval $[0.3, 2.0]$, and filtering out the very coarse meshes of the first few adaptive iterations of the "square" cases, the effectivity indices are all within the interval $[0.5, 2.0]$. This means that we at most over- or underestimate the error by a factor 2.

6 Acknowledgements

This research has been supported by EU-FET grant EUNISON 308874, the European Research Council, the Swedish Foundation for Strategic Research, the Swedish Research Council and the Basque Excellence Research Center (BERC) program by the Basque Government.

References

1. Wolfgang Bangerth and Rolf Rannacher. Finite element approximation of the acoustic wave equation: Error control and mesh adaptation. *East West Journal of Numerical Mathematics*, 7(4):263–282, 1999.
2. Roland Becker and Rolf Rannacher. A feed-back approach to error control in adaptive finite element methods: Basic analysis and examples. *East-West J. Numer. Math.*, 4:237–264, 1996.
3. Roland Becker and Rolf Rannacher. An optimal control approach to a posteriori error estimation in finite element methods. *Acta Numerica*, 10:1–102, 5 2001.
4. Roland Becker and Rolf Rannacher. A posteriori error estimation in finite element methods. *Acta Numer.*, 10:1–103, 2001.
5. A. C. Brenner and L. R. Scott. *The Mathematical Theory of Finite Element Methods*. Springer-Verlag, 1994.
6. E. Burman. Adaptive finite element methods for compressible two-phase flow. *Meth. Mod. Meth. App. Sci.*, 10(7):963–989, 2000.
7. M Crouzeix and V Thomée. The stability in l_p and w_pˆ1 of the l_2-projection onto finite element function spaces. *Mathematics of Computation*, pages 521–532, 1987.
8. Kenneth Eriksson, Don Estep, Peter Hansbo, and Claes Johnson. Introduction to adaptive methods for differential equations. *Acta Numer.*, 4:105–158, 1995.
9. Kenneth Eriksson, Don Estep, Peter Hansbo, and Claes Johnson. *Computational Differential Equations*. Cambridge University Press New York, 1996.
10. Kenneth Eriksson and Claes Johnson. An adaptive finite element method for linear elliptic problems. *Math. Comp.*, 50:361–383, 1988.
11. Donald Estep. A short course on duality, adjoint operators, greens functions, and a posteriori error analysis. *Lecture Notes*, 2004.
12. Michael B. Giles and Endre Süli. Adjoint methods for pdes: a posteriori error analysis and postprocessing by duality. *Acta Numerica*, 11:145–236, 1 2002.
13. Johan Hoffman, Johan Jansson, Rodrigo Vilela de Abreu, Niyazi Cem Degirmenci, Niclas Jansson, Kaspar Müller, Murtazo Nazarov, and Jeannette Hiromi Spühler. Unicorn: Parallel adaptive finite element simulation of turbulent flow and fluid-structure interaction for deforming domains and complex geometry. *Computers and Fluids*, 2012.
14. Johan Hoffman, Johan Jansson, Niclas Jansson, and Rodrigo Vilela de Abreu. Time-resolved adaptive fem simulation of the dlr-f11 aircraft model at high reynolds number. *Proceedings for AIAA SciTech 52nd Aerospace Sciences Meeting*, 2014.
15. Johan Jansson, Johan Hoffman, , Jeannette Spuhler, and Cem Degirmenci. Adaptive error control in finite element methods using the error representation as error indicator. *Technical Report KTH-CTL, Computational Technology Laboratory*, 2013.
16. D Pardo, L Demkowicz, C Torres-Verdin, and M Paszynski. A self-adaptive goal-oriented¡ i¿ hp¡/i¿-finite element method with electromagnetic applications. part ii: Electrodynamics. *Computer methods in applied mechanics and engineering*, 196(37):3585–3597, 2007.
17. M-C. Rivara. Local modification of meshes for adaptive and/or multigrid finite-element methods. *Journal of Computational and Applied Mathematics*, 36(1):78–89, 1992.
18. Marie E Rognes and Anders Logg. Automated goal-oriented error control i: Stationary variational problems. *SIAM Journal on Scientific Computing*, 35(3):C173–C193, 2013.

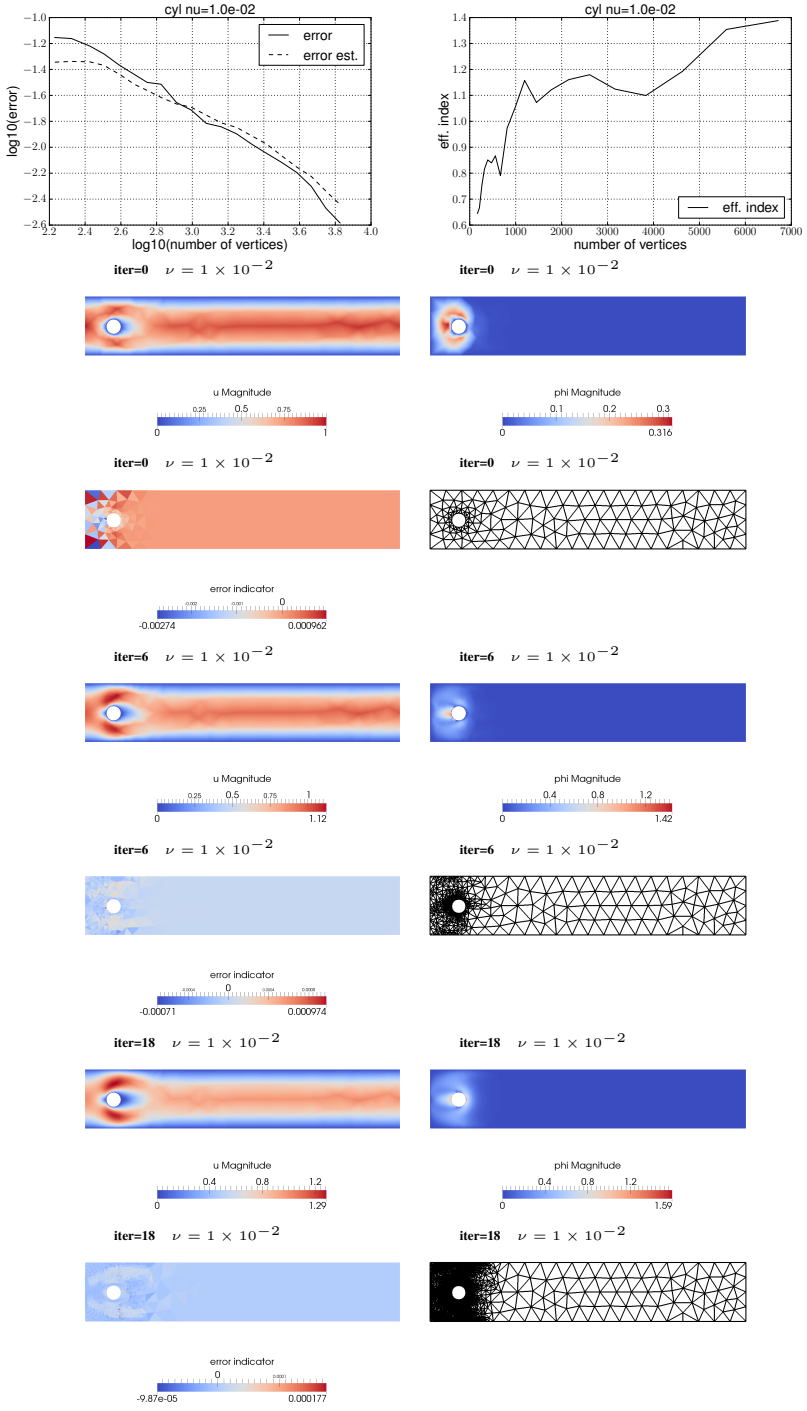

Fig. 3 Plots for representation adaptivity with pressure drag as target output applied to 2D incompressible Navier-Stokes flow around a cylinder with viscosity $\nu = 1 \times 10^{-2}$. Graph of error estimate vs. error and effectivity index $\frac{|r(U,\Phi)|}{|M(e)|}$ (upper) and velocity, dual velocity, error indicator function and mesh for selected adaptive iterations (lower).

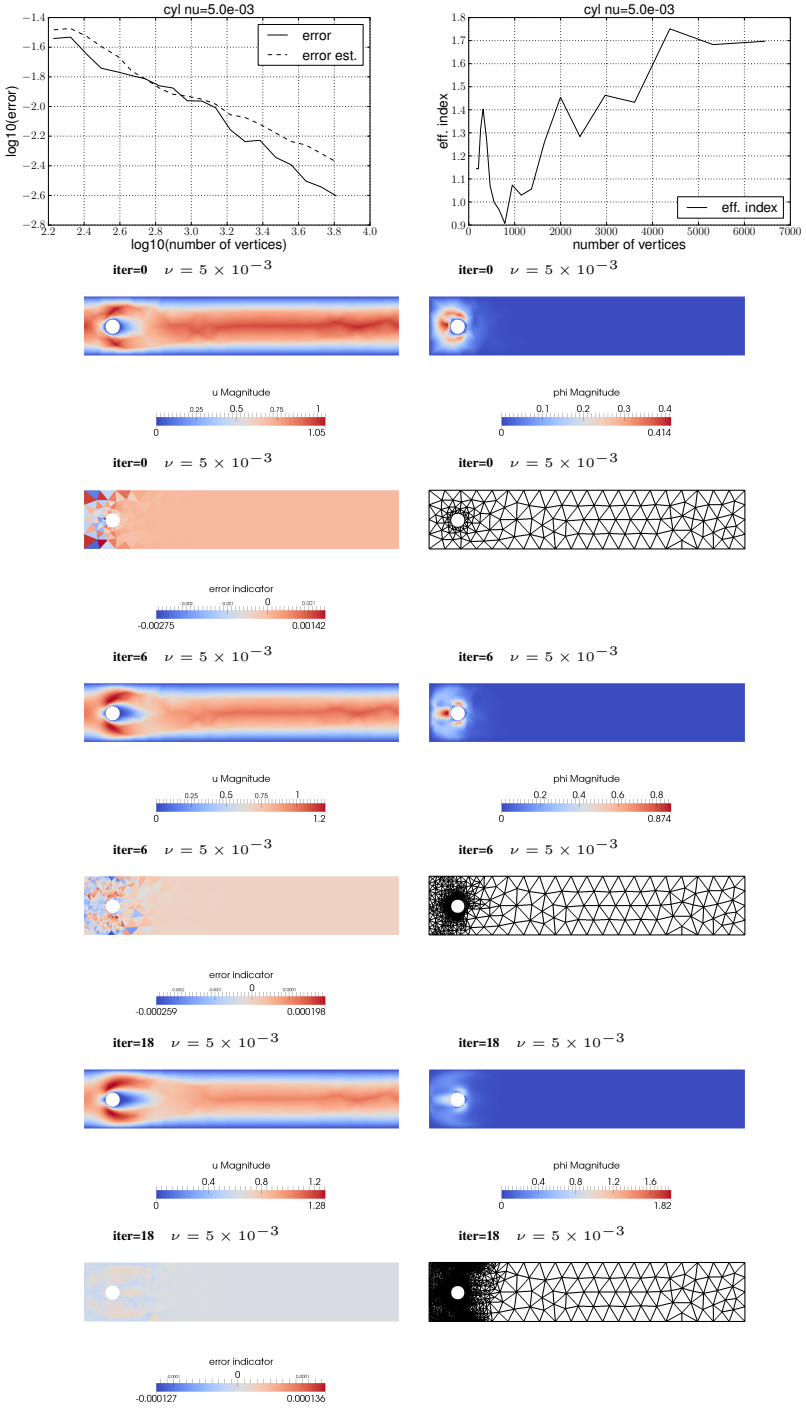

Fig. 4 Plots for representation adaptivity with pressure drag as target output applied to 2D incompressible Navier-Stokes flow around a cylinder with viscosity $\nu = 5 \times 10^{-3}$. Graph of error estimate vs. error and effectivity index $\frac{|r(U,\Phi)|}{|M(e)|}$ (upper) and velocity, dual velocity, error indicator function and mesh for selected adaptive iterations (lower).

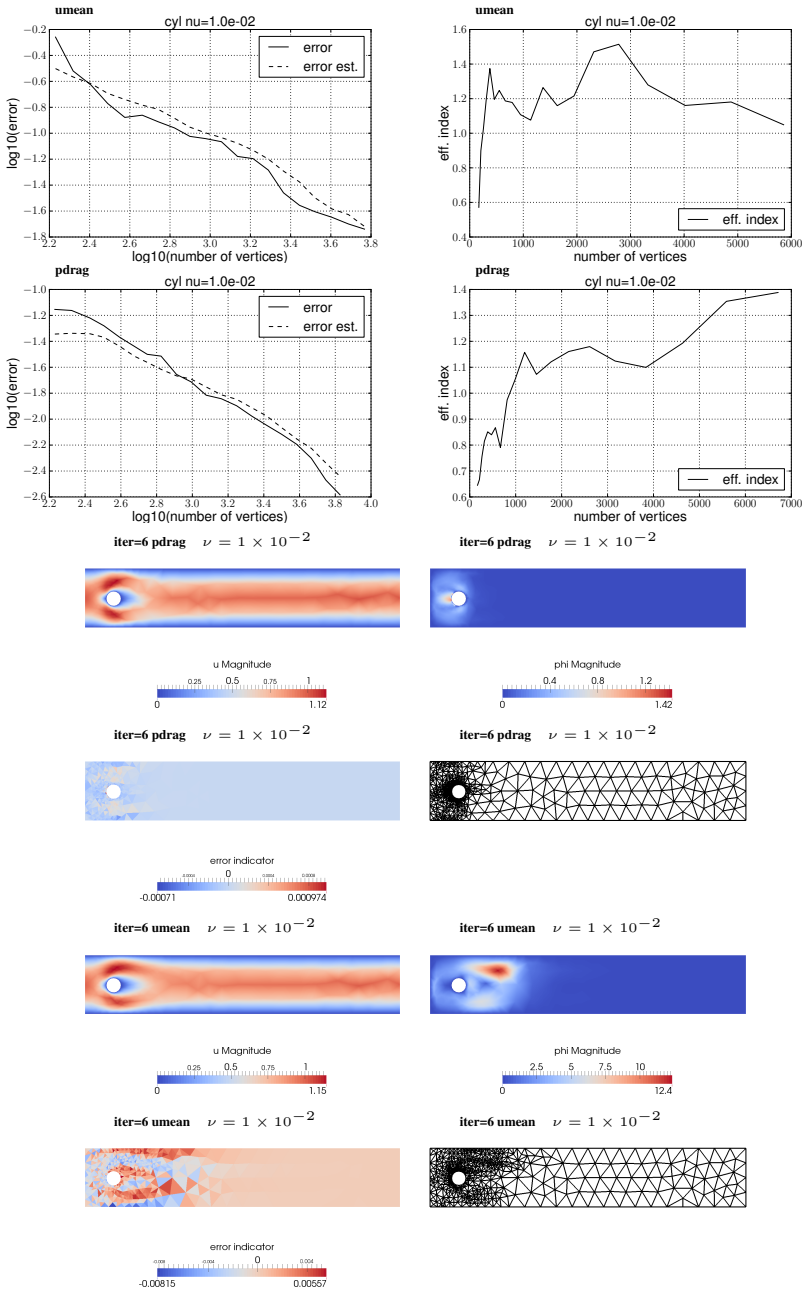

Fig. 5 Plots for representation adaptivity comparing pressure drag ("pdrag") and mean velocity weighted by a Gaussian function concentrated in a region ("umean") as target output applied to 2D incompressible Navier-Stokes flow around a cylinder with viscosity $\nu = 1 \times 10^{-2}$. Graph of error estimate vs. error and effectivity index $\frac{|r(U,\Phi)|}{|M(e)|}$ (upper) and velocity, dual velocity, error indicator function and mesh for selected adaptive iterations (lower).

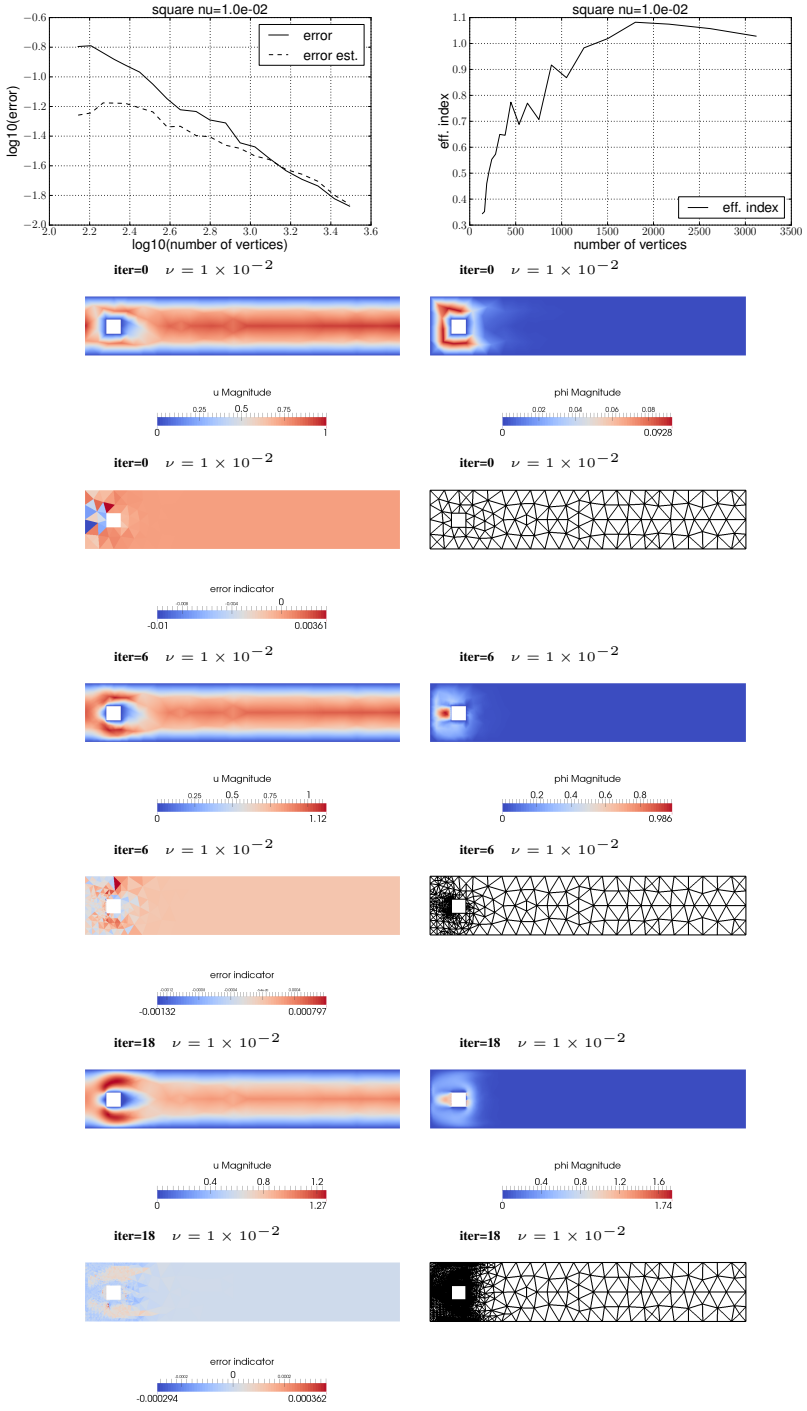

Fig. 6 Plots for representation adaptivity with pressure drag as target output applied to 2D incompressible Navier-Stokes flow around a square with viscosity $\nu = 1 \times 10^{-2}$. Graph of error estimate vs. error and effectivity index $\frac{|r(U,\Phi)|}{|M(e)|}$ (upper) and velocity, dual velocity, error indicator function and mesh for selected adaptive iterations (lower).

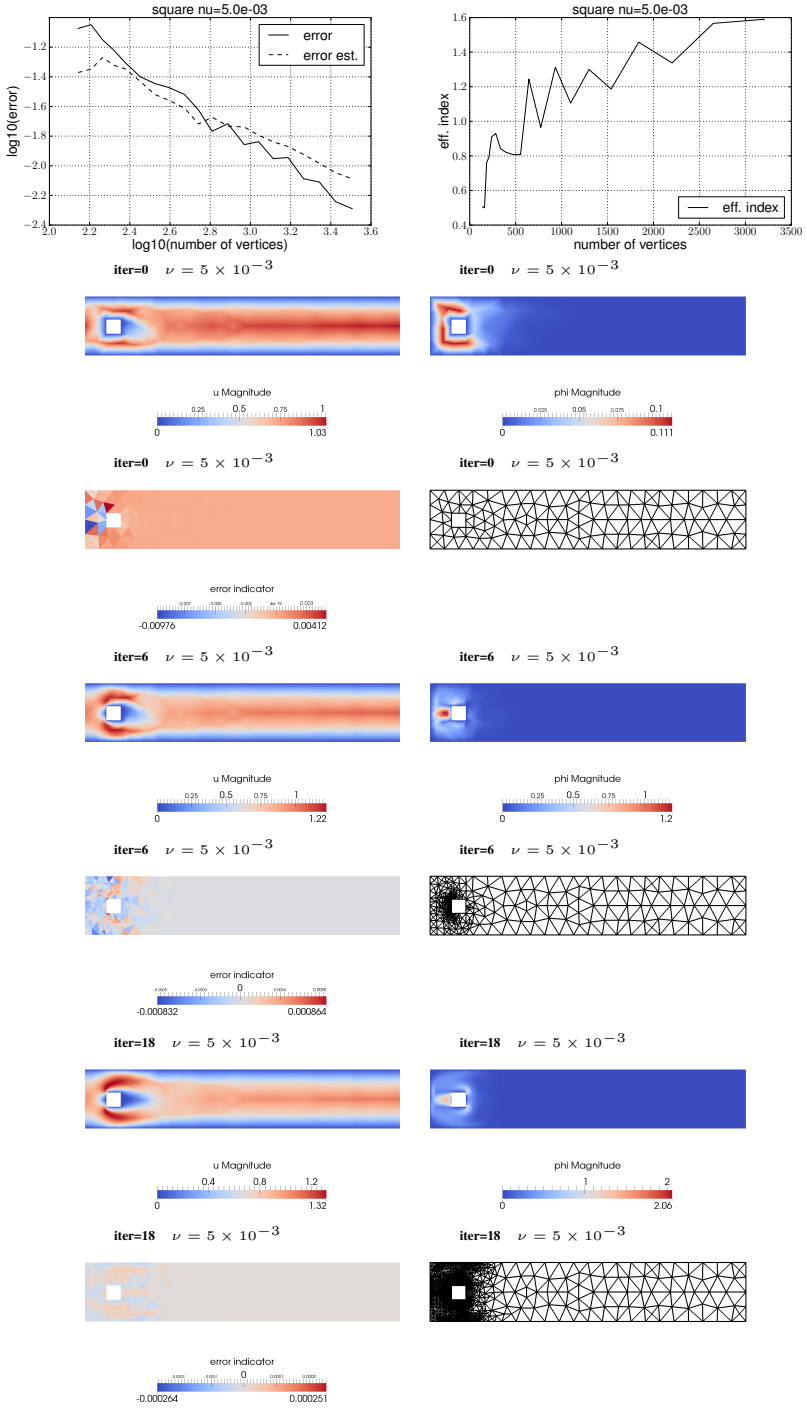

Fig. 7 Plots for representation adaptivity with pressure drag as target output applied to 2D incompressible Navier-Stokes flow around a square with viscosity $\nu = 5 \times 10^{-3}$. Graph of error estimate vs. error and effectivity index $\frac{|r(U,\Phi)|}{|M(e)|}$ (upper) and velocity, dual velocity, error indicator function and mesh for selected adaptive iterations (lower).

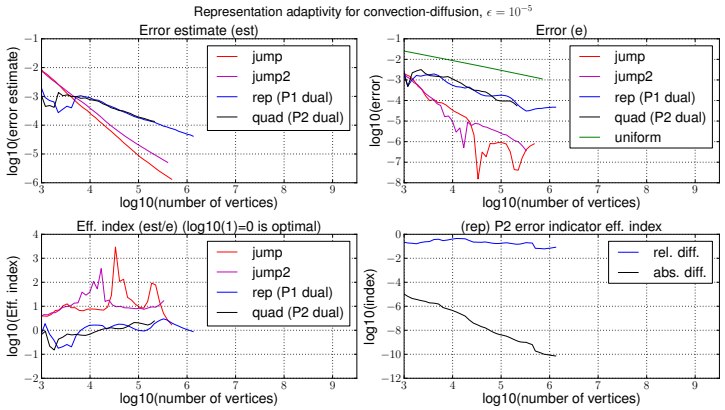

Fig. 8 Graphs of error control quantities for the convection-diffusion test problem (annotated in the graphs).

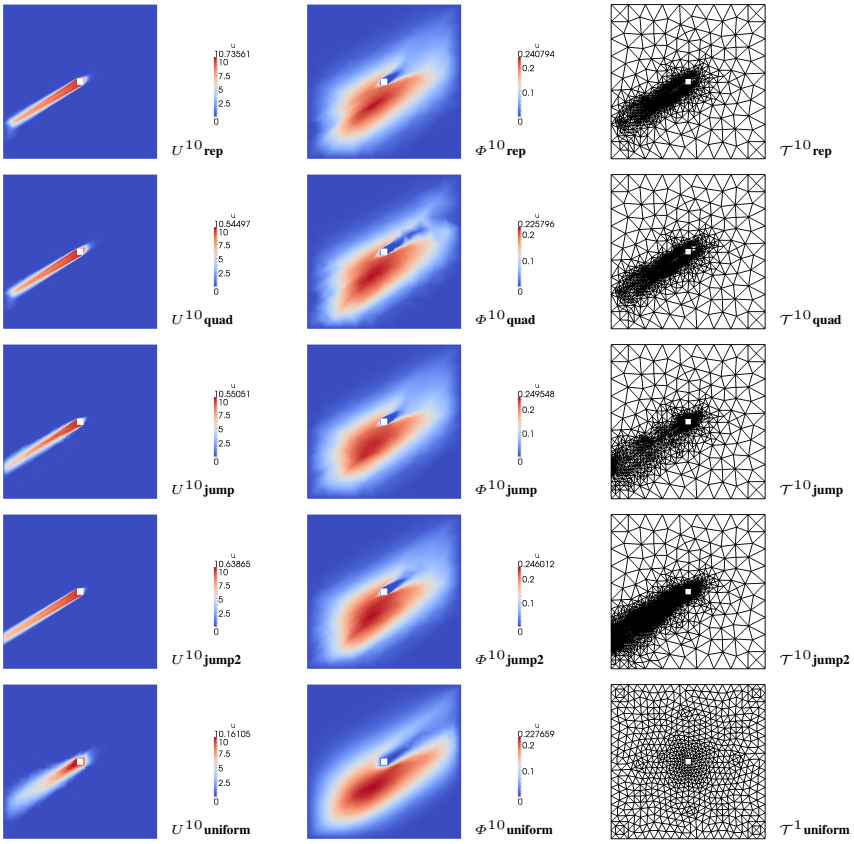

Fig. 9 Comparison of solution U and dual Φ for all methods for the convection-diffusion test problem with $\epsilon = 10^{-1}, |\beta| = 1.171$

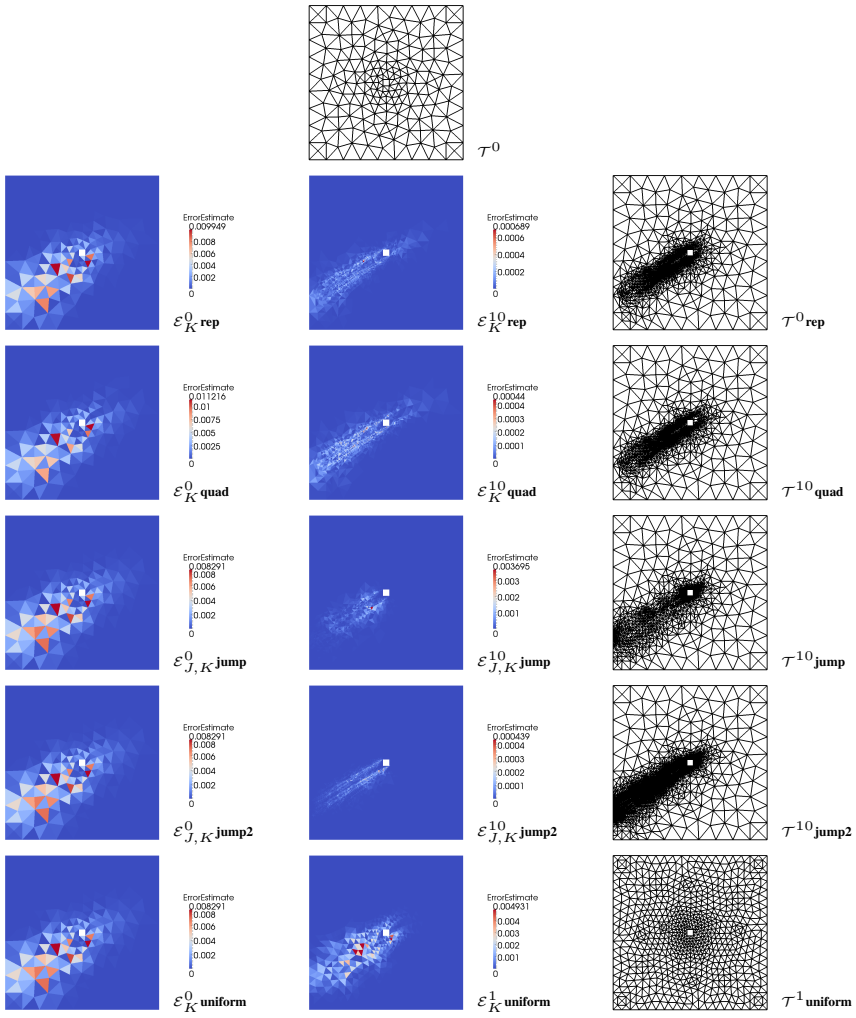

Fig. 10 Comparison of adaptive error control quantitites and meshes for all methods for the convection-diffusion test problem with $\epsilon = 10^{-5}$, $|\beta| = 1.171$